

Supporting Information

Construction of a Controllable Self-Assembled Dual-Mode Al³⁺ Sensor Based on Substituent Effects of Flavonoids

Ping Yang,* Wen Liu, Yuanlin Zhang, Haoyuan Lv, Kuiliang Li* and Duoduo Hu

Corresponding Authors : Ping Yang(pyang8066@163.com);

Kuiliang Li(likuil@mail.ustc.edu.cn)

School of Chemical Blasting Engineering, Anhui University of Science and Technology, Huainan, Anhui, 232001, P. R. China; State Key Laboratory of Safe Mining of Deep Coal and Environmental Protection, Huainan 232000, P. R. China.

Table of Contents

1. The synthesis route of compounds	1
1.1 Synthesis of 3HF	1
1.2 Synthesis of BHF	1
1.3 Synthesis of BCN	2
1.4 Synthesis of BCA	2
1.5 Synthesis of BBCN	3
Figure S1. FTIR spectrum changes before and after BCN addition of Al³⁺.	4
Figure S2. FTIR spectrum changes before and after BBCN addition of Al³⁺.	4
Figure S3. ¹H NMR spectrum of 3HF in DMSO-d⁶ solvent.	5
Figure S4. ¹H NMR spectrum of BHF in DMSO-d⁶ solvent.	5
Figure S5. ¹H NMR spectrum of BCA in chloroform-d solvent.	6
Figure S6. ¹³C NMR spectrum of BCA in chloroform-d solvent.	6
Figure S7. ¹H NMR spectrum of BCN in chloroform-d solvent.	7
Figure S8. ¹³C NMR spectrum of BCN in chloroform-d solvent.	7
Figure S9. ¹H NMR spectrum of BBCN in chloroform-d solvent.	8
Figure S10. ¹³C NMR spectrum of BBCN in DMSO-d⁶ solvent.	8
Figure S11. HRMS of 3HF(ESI+).	9
Figure S12. HRMS of BHF(ESI+).	9
Figure S13. HRMS of BCA(ESI+).	10
Figure S14. HRMS of BCN(ESI+).	10
Figure S15. HRMS of BBCN(ESI+).	11
Figure S16. UV-Vis spectra of 3HF (a), BCA (b), BCN (c), and BBCN (d) before and after adding 100μM of Al³⁺ in solution (H₂O:THF = 9:1).	11
Figure S17. Fluorescence spectra of 3HF (a), BCA (b), BCN (c), and BBCN (d) before and after adding 100μM of Al³⁺ in solution (H₂O:THF = 9:1).	12

Figure S18. Fluorescence spectra of BCN (a) and 3HF (b) at low concentrations of Al³⁺	12
Figure S19. Size distribution(DLS) of 3HF (a), BCA (b), BCN (c), and BBCN (d) before and after adding 100μM of Al³⁺ in solution (H₂O:THF = 9:1).	13
Figure S20. (a) XRD pattern of BCN-Al³⁺ and (b) XRD pattern of BBCN-Al³⁺ complexes	13
Figure S21. Photographs of fluorescence responses at 365 nm after adding 100 μM different metal ions to BCN aqueous solution (H₂O:THF = 9:1).	14
Figure S22. Fluorescence spectra of 3HF aqueous solution (H₂O:THF = 9:1) after addition of 100μM of various metal ions.	14
Figure S23. The photophysical behaviors of 3HF and BCN in solvents, including non-polar solvent (toluene), polar aprotic solvent (THF), and polar protic solvent (methanol).	15
Figure S24. Color change of the system before and after adding different concentrations (0–100–500 μM) of Al³⁺ to a BCN (50 μM) aqueous solution.	15
Figure S25. (a) Job curve of BCA binding to Al³⁺ in aqueous solution at a 2:1 molar ratio (all dissolution systems were H₂O:THF = 9:1); (b) Benesi-Hildebrand curve used to determine the binding constant.	16
Figure S26. (a) Job curve of BCN binding to Al³⁺ in aqueous solution at a 2:1 molar ratio (all dissolution systems were H₂O:THF = 9:1); (b) Benesi-Hildebrand curve used to determine the binding constant.	16
Figure S27. (a) Job curve of BBCN binding to Al³⁺ in aqueous solution at a 2:1 molar ratio (all dissolution systems were H₂O:THF = 9:1); (b) Benesi-Hildebrand curve used to determine the binding constant.	17
Figure S28. HRMS of 2BCN+Al³⁺ (ESI+).	17
Figure S29. TD-DFT simulated absorption spectra and assignments of major electronic transitions for BCA(a), BCA-Al³⁺(b), BCN(c), and BCN-Al³⁺(d).	18

1. The synthesis route of compounds

1.1 Synthesis of 3HF

In a 25 mL round-bottom flask equipped with a magnetic stirrer, were added 2-hydroxyacetophenone (1.66 mmol, 0.202 mL), benzaldehyde (1.66 mmol, 0.17 mL), and a methanolic solution of sodium hydroxide (0.2 g, 5 mmol, dissolved in 10 mL of methanol). The pale yellow mixture was refluxed at 70 °C until the color changed to orange-yellow, which took approximately 3 hours. After cooling the reaction mixture to room temperature, a 0.5 M ice-cold aqueous sodium hydroxide solution (10 mL) was added, followed by 30% hydrogen peroxide (0.8 mL). The resulting mixture was stirred in an ice bath for 2–3 hours, until a pale yellow flocculent precipitate formed. The mixture was then titrated with a 1.0 M hydrochloric acid solution (10 mL). When the pH reached 7.5, the flocculent precipitate settled and separated distinctly from the solution. The precipitate was collected by filtration to afford the pale yellow solid 3-hydroxyflavone (3HF) (0.36 g, 90% yield).

^1H NMR (400 MHz, DMSO- d_6) δ : 9.67 (s, 1H), 8.34–8.19 (m, 2H), 8.14 (dd, J = 8.0, 1.6 Hz, 1H), 7.86–7.74 (m, 2H), 7.58 (t, J = 7.4 Hz, 2H), 7.54–7.44 (m, 2H). HRMS (ESI) m/z : $[\text{M}+\text{H}]^+$ Calcd for $\text{C}_{15}\text{H}_{11}\text{O}_3$ 239.0612; Found 239.0734.

1.2 Synthesis of BHF

In a 25 mL round-bottom flask equipped with a magnetic stirrer, were added 2-hydroxy-5-bromoacetophenone (1.66 mmol, 357 mg), benzaldehyde (1.66 mmol, 0.17 mL), and a methanolic solution of sodium hydroxide (0.2 g, 5 mmol, dissolved in 10 mL of methanol). The pale yellow mixture was refluxed at 70 °C until the color changed to orange-red, a process that took approximately 2.5 hours. The subsequent procedures were identical to those described for the synthesis of 3HF, affording a yellow solid 6-bromo-3-hydroxyflavone (BHF) (0.49 g, 91% yield).

^1H NMR (400 MHz, DMSO- d_6) δ 8.41 (dq, J = 7.4, 1.7 Hz, 2H), 8.13 – 8.07 (m, 1H), 7.72 (dd, J = 3.7, 2.0 Hz, 2H), 7.52 – 7.47 (m, 2H), 7.41 – 7.39 (m, 1H). HRMS (ESI) m/z : $[\text{M}+\text{H}]^+$ (79Br) Calcd for $\text{C}_{15}\text{H}_{10}\text{BrO}_3$ 316.9807; Found 316.9774.

1.3 Synthesis of BCN

To a mixture of 2-(methylamino) benzoic acid (5 mmol, 0.76 g) and 3HF (5 mmol, 1.19 g) in 50 mL of dichloromethane (DCM), 4-dimethylaminopyridine (DMAP, 1 mmol, 0.122 g) and 1-ethyl-3-(3-dimethylaminopropyl)carbodiimide hydrochloride (EDC.HCl, 5.5 mmol, 1.05 g) were added under an ice bath. The reaction mixture was stirred at room temperature for 12 hours. Subsequently, the mixture was extracted with 40 mL of 0.5 M hydrochloric acid (HCl) solution and DCM (30 mL × 2). The combined organic layers were washed successively with 1% aqueous sodium bicarbonate (NaHCO₃) solution and saturated sodium chloride (NaCl) solution, dried over anhydrous magnesium sulfate (MgSO₄), filtered, and concentrated under reduced pressure to afford a crude product. Further purification by column chromatography furnished a white powder BCN (1.48 g, 81% yield).

¹H NMR (400 MHz, Chloroform-d) δ: 8.29 (dd, J = 8.0, 1.7 Hz, 1H), 8.14 (dd, J = 8.0, 1.7 Hz, 1H), 8.00-7.92 (m, 2H), 7.72 (ddd, J = 8.7, 7.1, 1.7 Hz, 1H), 7.61-7.58 (m, 1H), 7.56-7.37 (m, 6H), 6.72-6.63 (m, 2H), 2.88 (s, 3H). ¹³C NMR (101 MHz, Chloroform-d) δ: 172.52, 165.76, 156.25, 155.66, 152.82, 135.69, 133.91, 133.87, 132.41, 131.19, 130.12, 128.72, 128.62, 128.33, 127.75, 126.23, 125.13, 123.66, 118.10, 114.68, 110.90, 108.07, 29.56. HRMS (ESI) m/z:[M+H]⁺ Calcd for C₂₃H₁₈NO₄ 372.1211; Found 372.1254.

1.4 Synthesis of BCA

DMAP (4-dimethylaminopyridine) (1 mmol, 0.122 g) and EDC.HCl (5.5 mmol, 1.05 g) were added to a mixture of benzoic acid (5 mmol, 0.61 g) and 3HF (5 mmol, 1.19 g). 50 mL of DCM was added over an ice bath. Subsequent procedures were identical to those in BCN, yielding a pale yellow powder of 3-benzoyloxyflavone (BCA) (1.28 g, 75%).

¹H NMR (400 MHz, Chloroform-d) δ: 8.40 (d, J = 2.5 Hz, 1H), 8.19 (d, J = 8.1 Hz, 2H), 7.91 (dd, J = 7.7, 1.9 Hz, 2H), 7.81 (dd, J = 8.9, 2.5 Hz, 1H), 7.67–7.62 (m, 1H), 7.60–7.40 (m, 7H). ¹³C NMR (101 MHz, Chloroform-d) δ: 170.94, 163.73, 156.71, 154.44, 136.99, 133.99, 133.97, 131.50, 130.56, 129.68, 128.79, 128.72, 128.68, 128.65, 128.44, 128.32, 127.92, 127.80, 127.76, 125.06, 120.10, 118.71. HRMS (ESI) m/z:[M+H]⁺ Calcd for C₂₂H₁₅O₄ 343.0965; Found 343.1014.

1.5 Synthesis of BBCN

To a mixture of 2-(methylamino)benzoic acid (5 mmol, 0.76 g) and BHF (5 mmol, 1.58 g), 4-dimethylaminopyridine (DMAP, 1 mmol, 0.122 g) and 1-ethyl-3-(3-dimethylaminopropyl)carbodiimide hydrochloride (EDC.HCl, 5.5 mmol, 1.05 g) were added. Thereafter, 50 mL of dichloromethane (DCM) was introduced under an ice bath. The subsequent procedures were identical to those described for the synthesis of BCN, affording a yellow powder 6-bromo-3-[2-(methylamino)benzoyloxy]flavone (BBCN) (1.8 g, 80% yield).

^1H NMR (400 MHz, Chloroform- d) δ : 8.40 (d, J = 2.5 Hz, 1H), 8.12 (dd, J = 8.1, 1.6 Hz, 1H), 7.93 (dd, J = 7.6, 2.1 Hz, 2H), 7.81 (dd, J = 8.9, 2.4 Hz, 1H), 7.58-7.41 (m, 6H), 6.75–6.65 (m, 2H), 2.89 (s, 3H). ^{13}C NMR (101 MHz, DMSO- d_6) δ : 170.24, 164.44, 156.23, 154.03, 152.17, 137.30, 136.07, 132.95, 131.71, 131.64, 129.08, 128.88, 128.46, 128.09, 127.64, 126.95, 124.24, 121.42, 118.12, 114.49, 111.29, 106.67, 29.19. HRMS (ESI) m/z : $[\text{M}+\text{H}]^+$ (79Br) Calcd for $\text{C}_{23}\text{H}_{17}\text{BrNO}_4$ 450.0325; Found 450.0347.

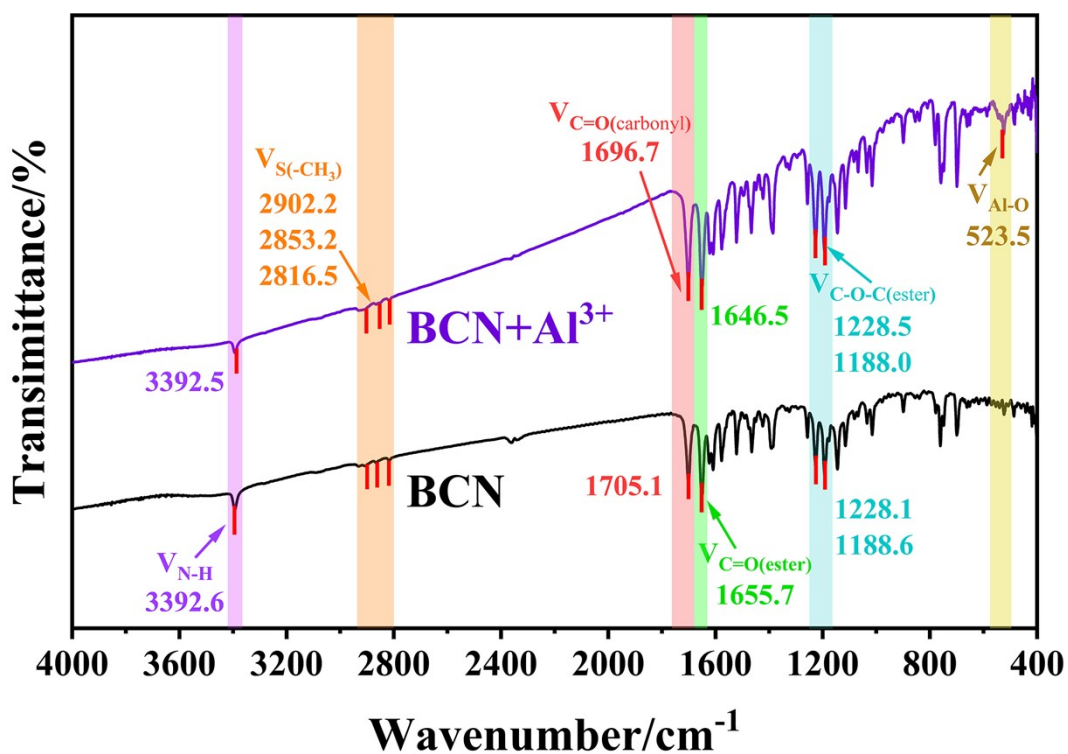


Figure S1. FTIR spectrum changes before and after BCN addition of Al³⁺.

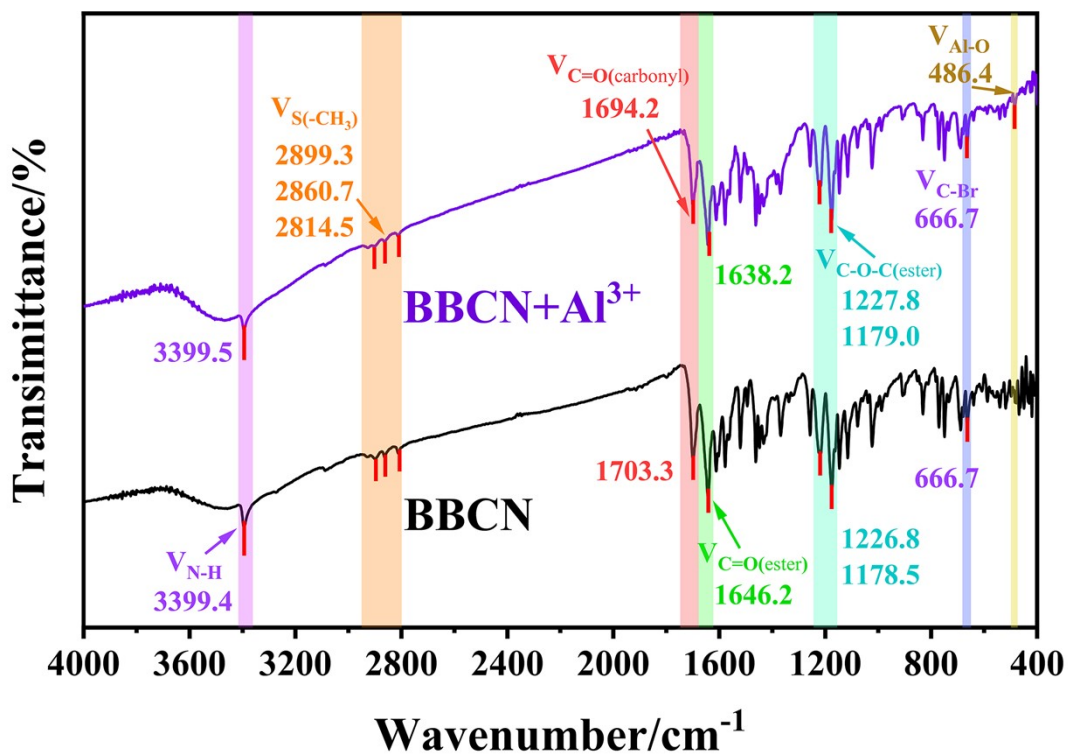


Figure S2. FTIR spectrum changes before and after BBCN addition of Al³⁺.

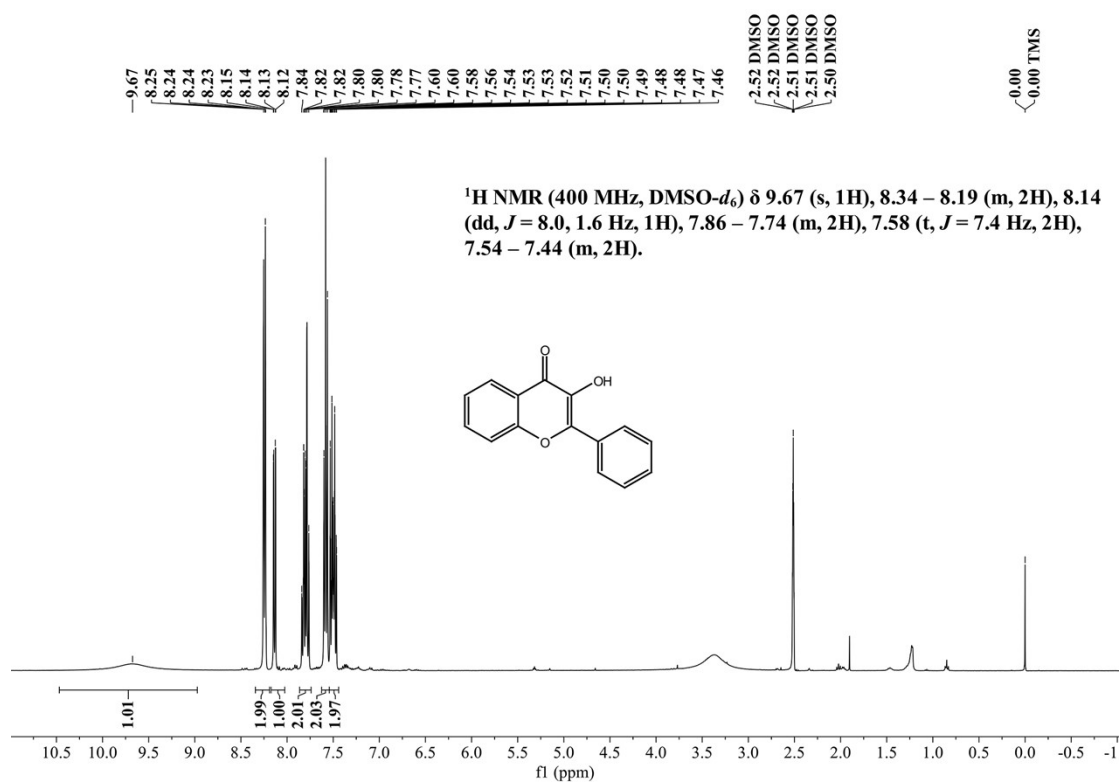


Figure S3. ¹H NMR spectrum of 3HF in DMSO-*d*₆ solvent. Signals at 3.3 ppm and 2.52 ppm are assigned to H₂O and DMSO, respectively.

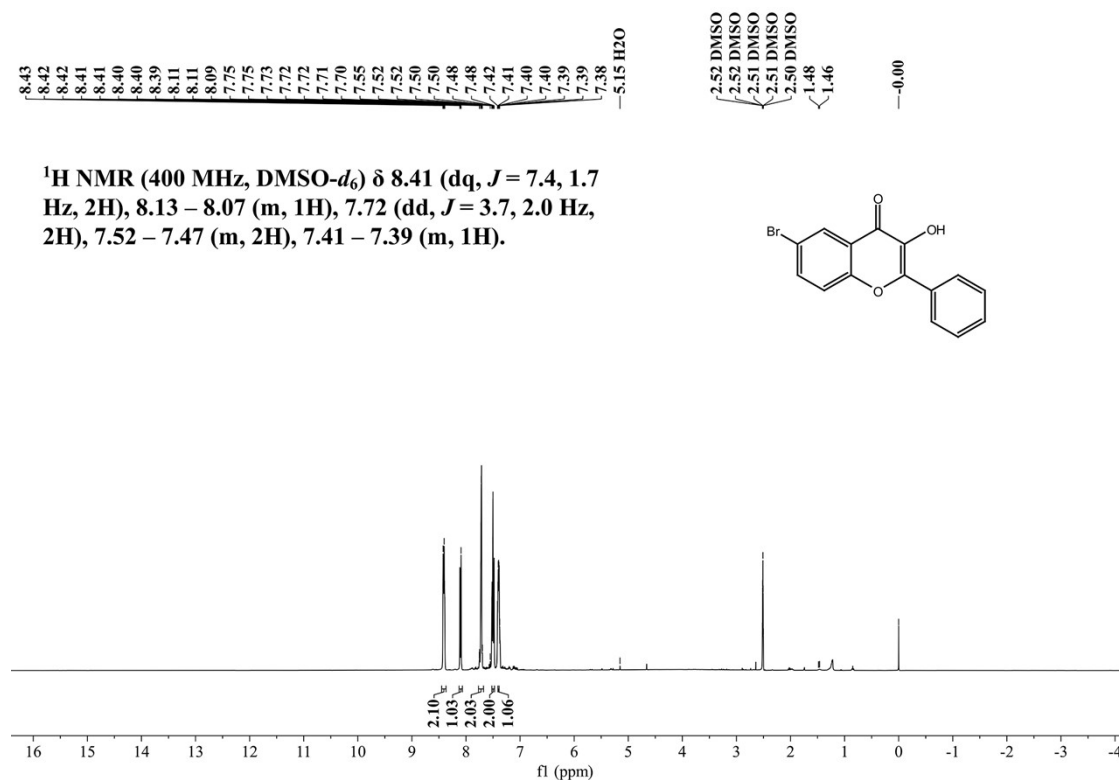


Figure S4. ¹H NMR spectrum of BHF in DMSO-*d*₆ solvent. Signal at 2.52 ppm is assigned to DMSO-*d*₆, respectively.

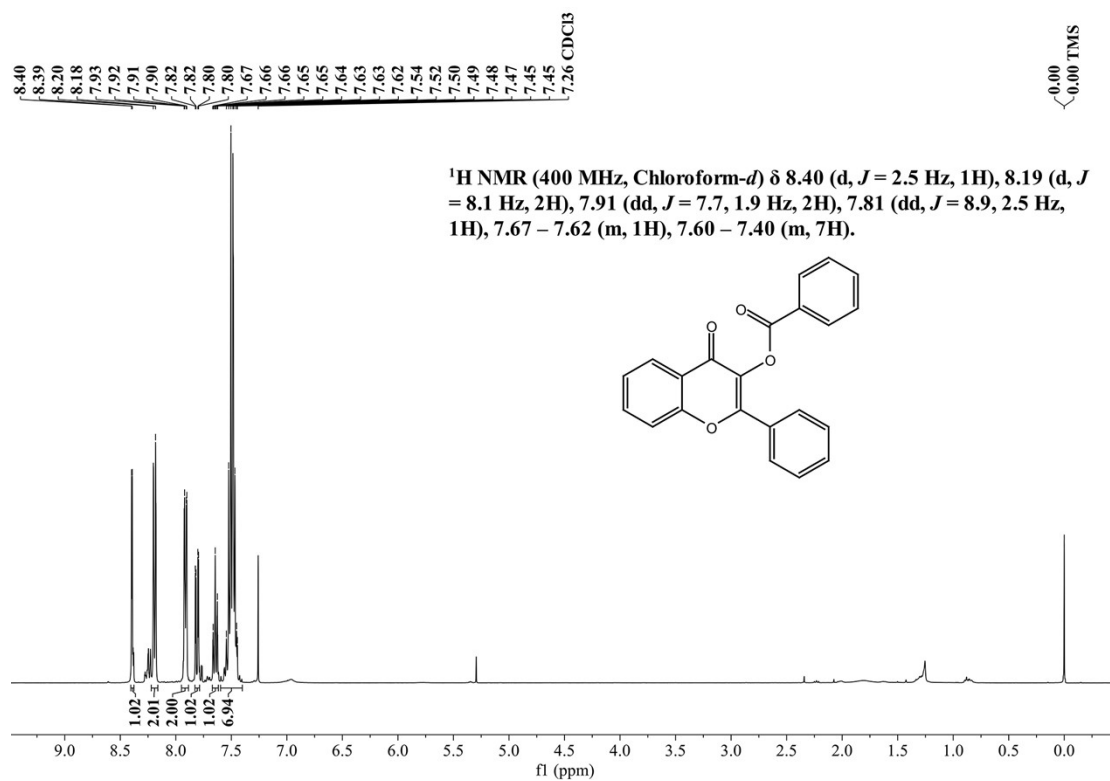


Figure S5. ¹H NMR spectrum of BCA in chloroform-*d* solvent. The signal at 7.26 ppm is assigned to chloroform-*d*.

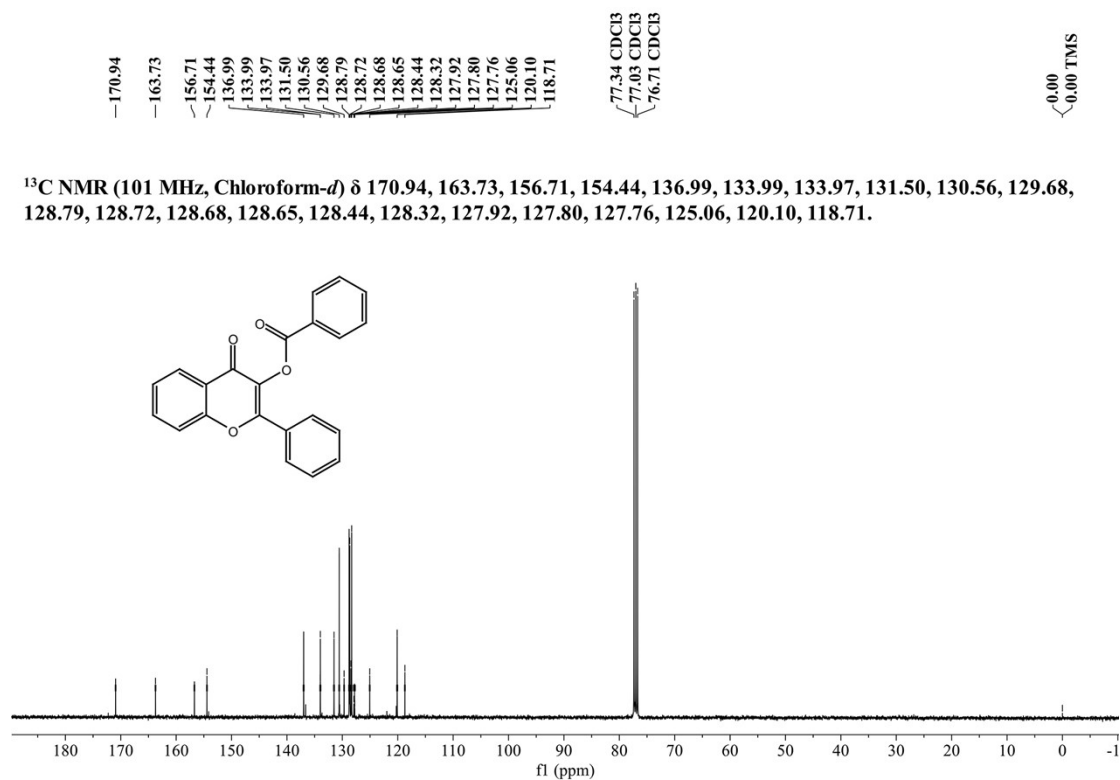


Figure S6. ¹³C NMR spectrum of BCA in chloroform-*d* solvent. The signal at 77.03 ppm is assigned to chloroform-*d*.

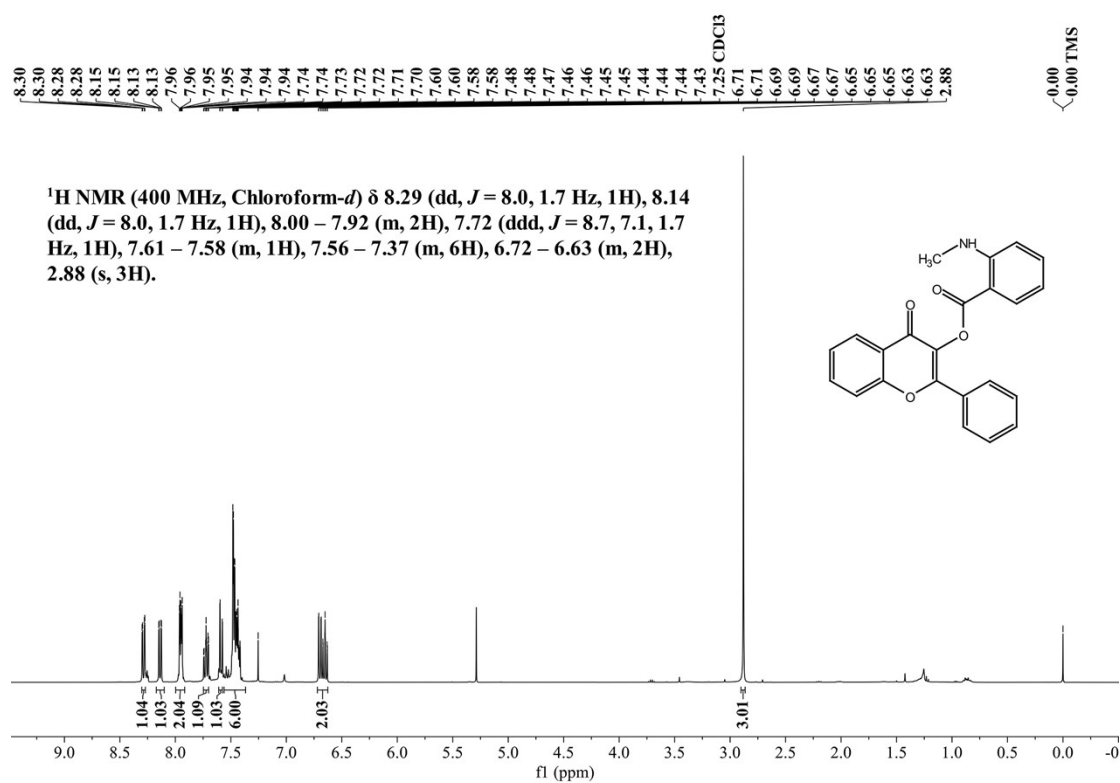


Figure S7. ¹H NMR spectrum of BCN in chloroform-*d* solvent. The signal at 7.25 ppm is assigned to chloroform-*d*.

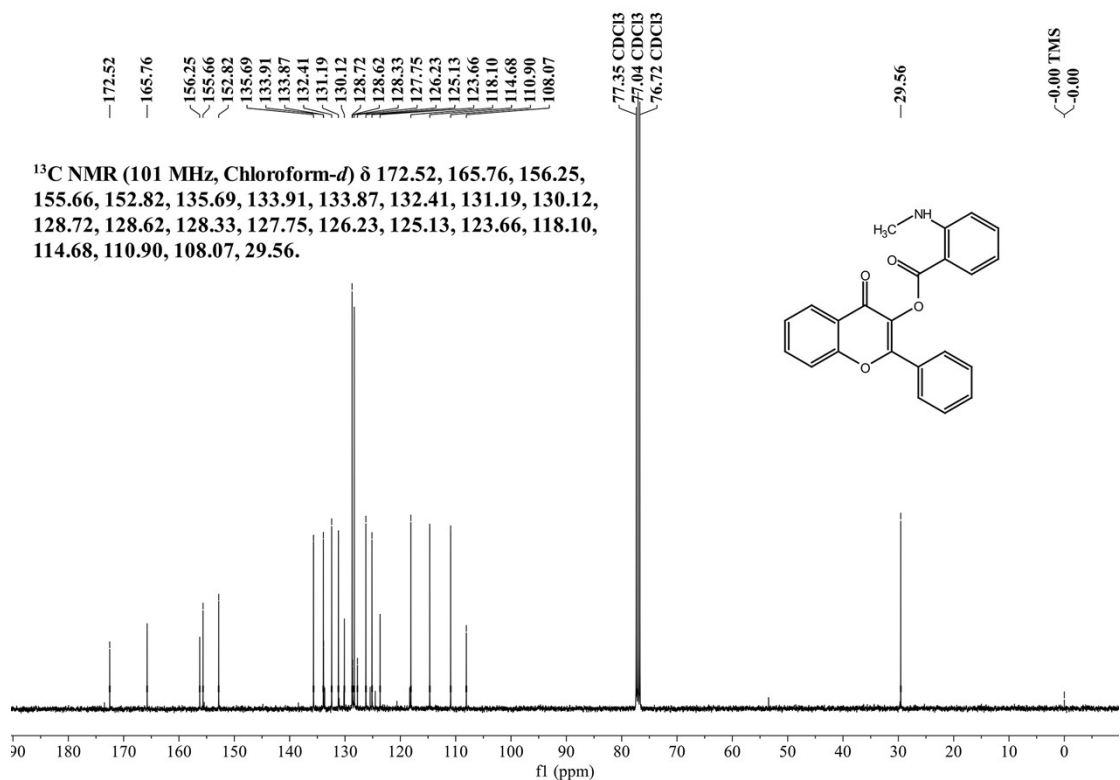


Figure S8. ¹³C NMR spectrum of BCN in chloroform-*d* solvent. The signal at 77.04 ppm is assigned to chloroform-*d*.

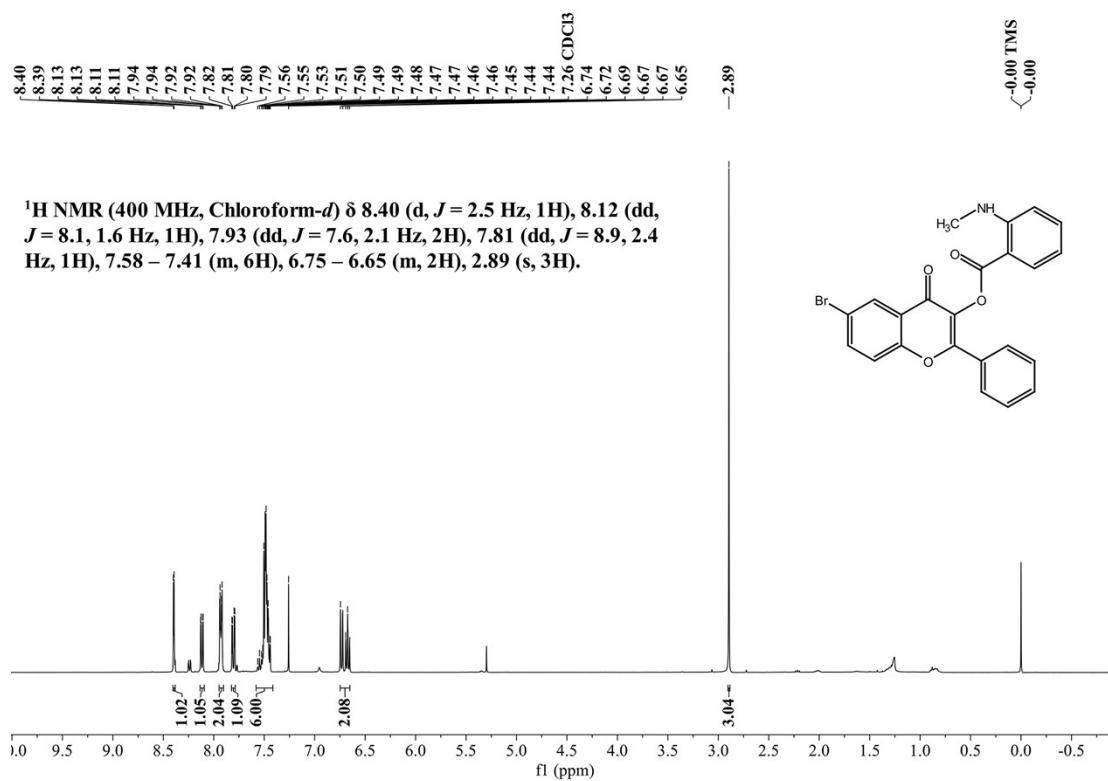


Figure S9. ¹H NMR spectrum of BBCN in chloroform-*d* solvent. The signal at 7.26 ppm is assigned to chloroform-*d*.

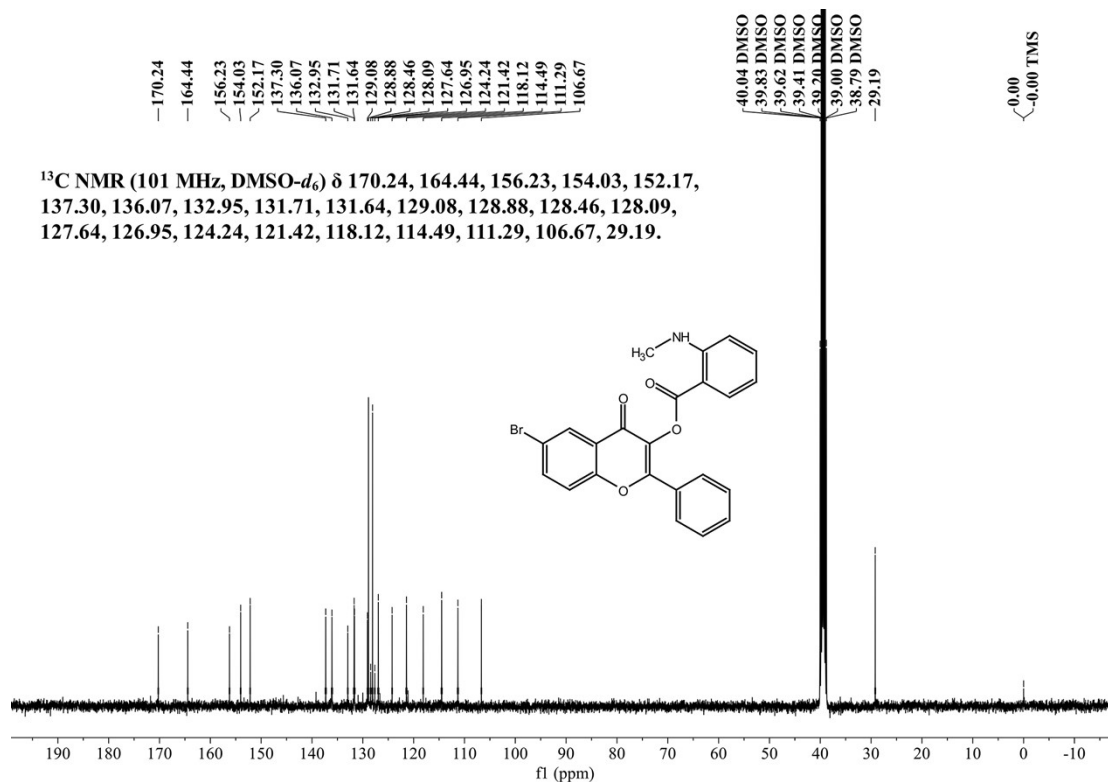


Figure S10. ¹³C NMR spectrum of BBCN in DMSO-*d*₆ solvent. The signal at 40 ppm is assigned to DMSO-*d*₆.

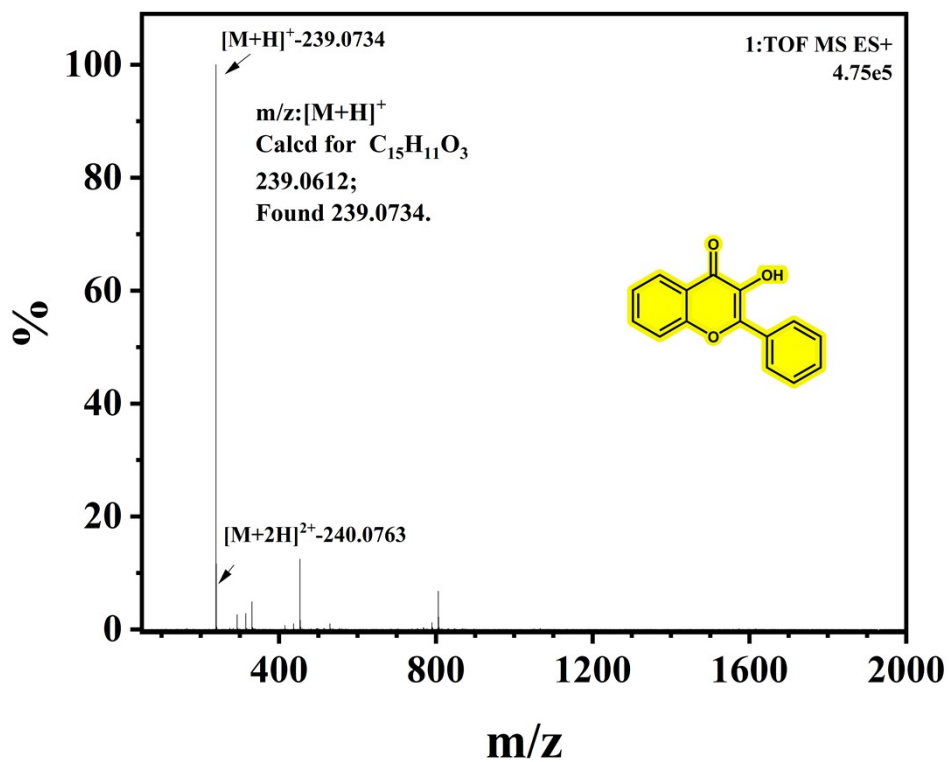


Figure S11. HRMS of 3HF(ESI+).

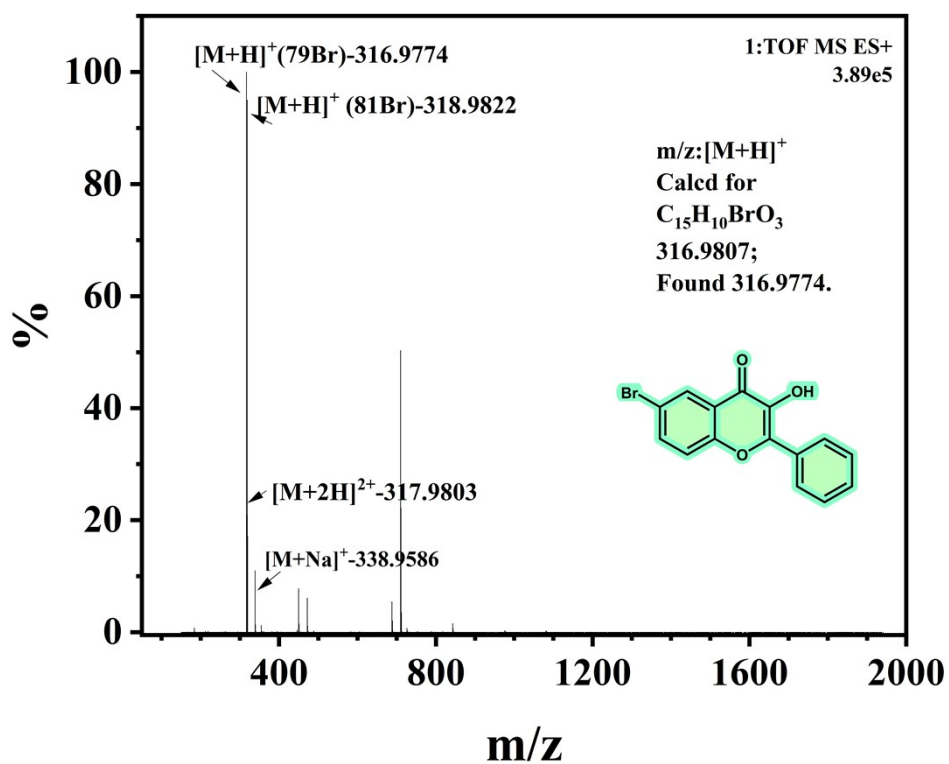


Figure S12. HRMS of BHF(ESI+).

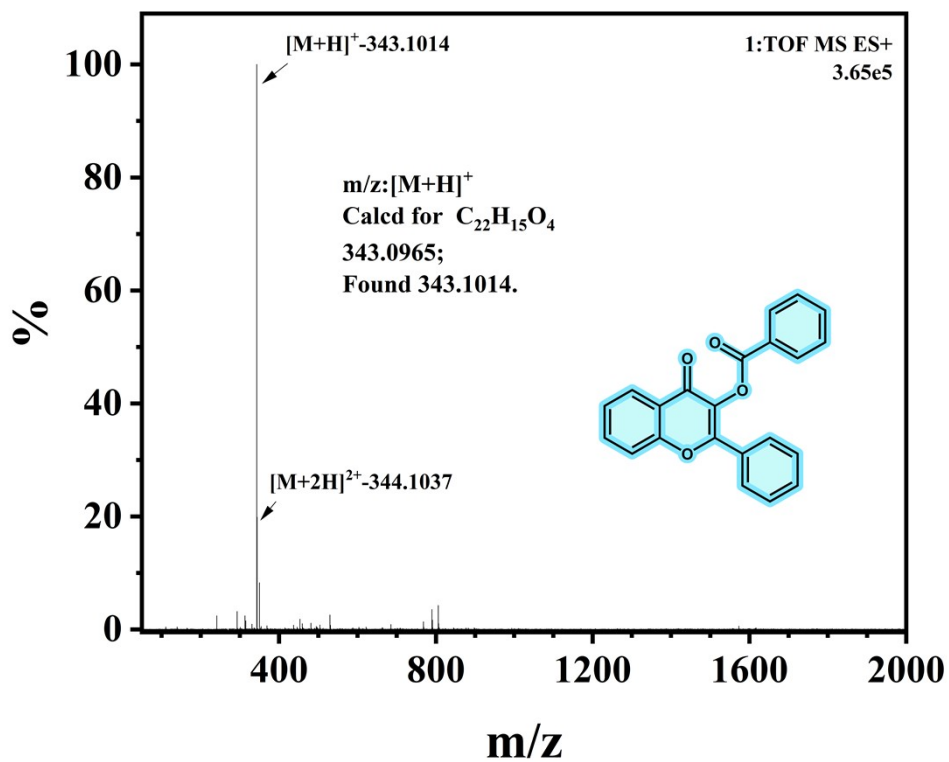


Figure S13. HRMS of BCA(ESI+).

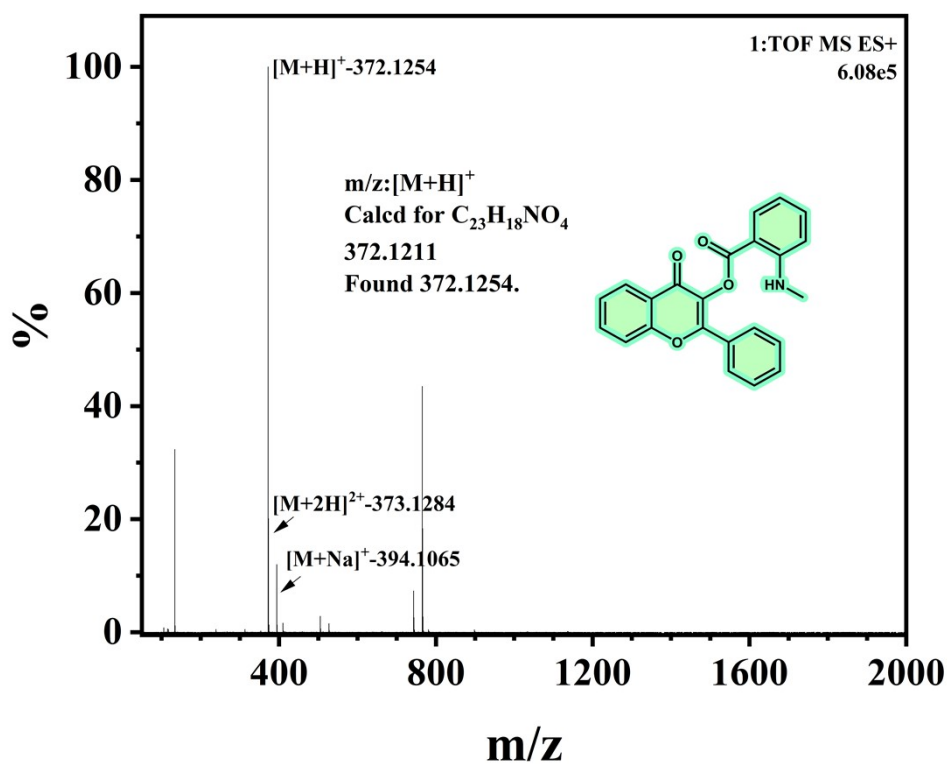


Figure S14. HRMS of BCN(ESI+).

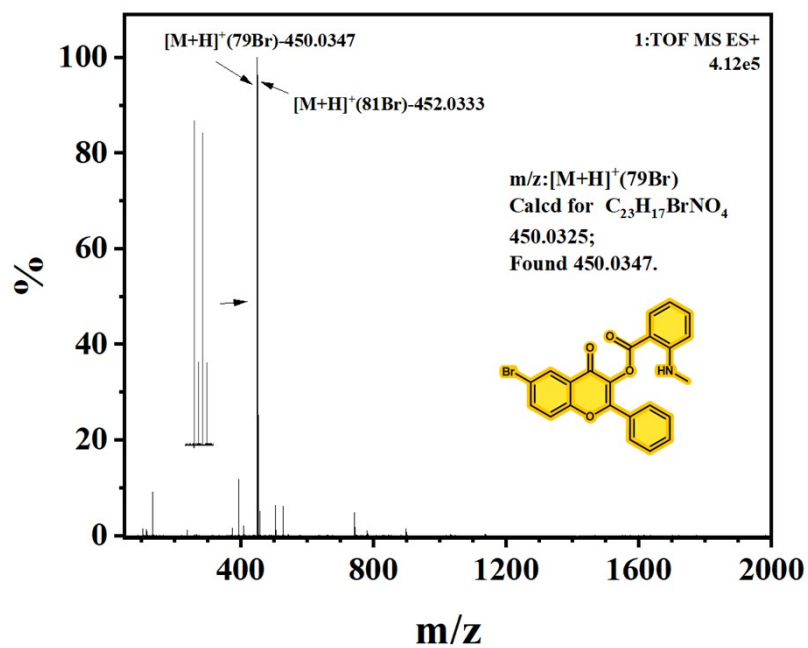


Figure S15. HRMS of BBCN(ESI+).

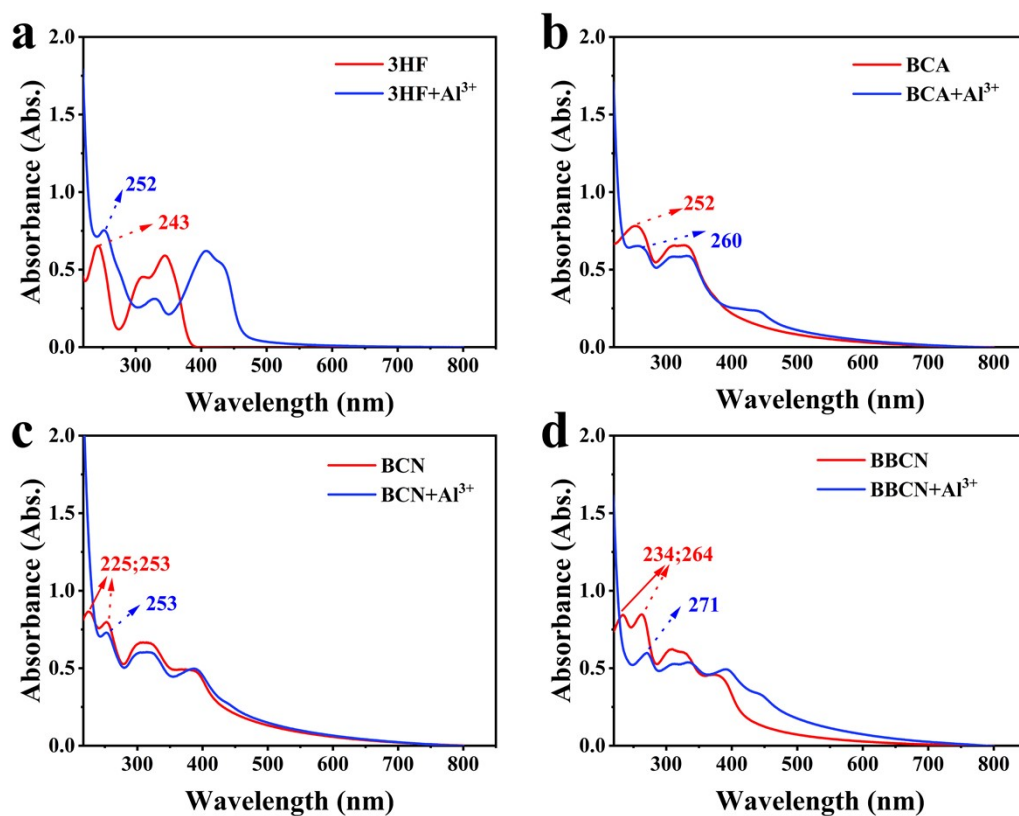


Figure S16. UV-Vis spectra of 3HF (a), BCA (b), BCN (c), and BBCN (d) before and after adding $100\mu M$ of Al^{3+} in solution ($H_2O:THF = 9:1$).

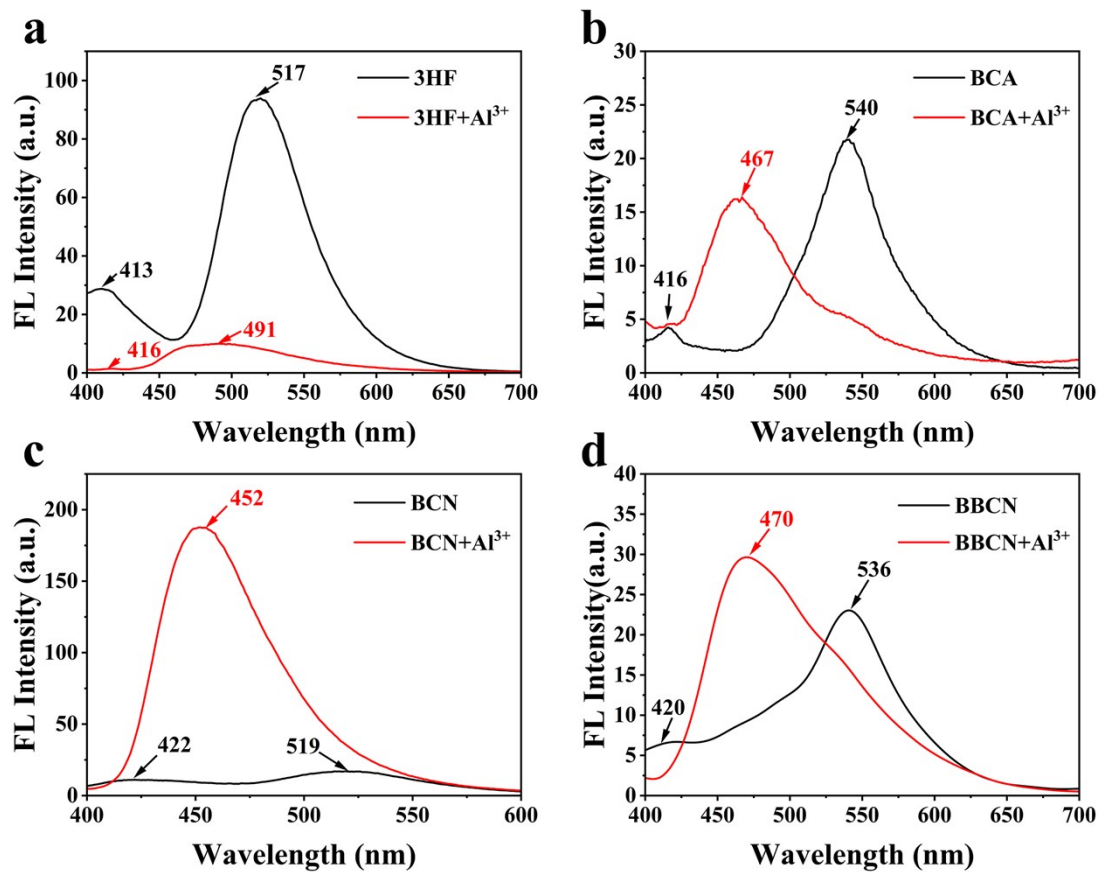


Figure S17. Fluorescence spectra of 3HF (a), BCA (b), BCN (c), and BBCN (d)

before and after adding 100 μM of Al³⁺ in solution (H₂O:THF = 9:1).

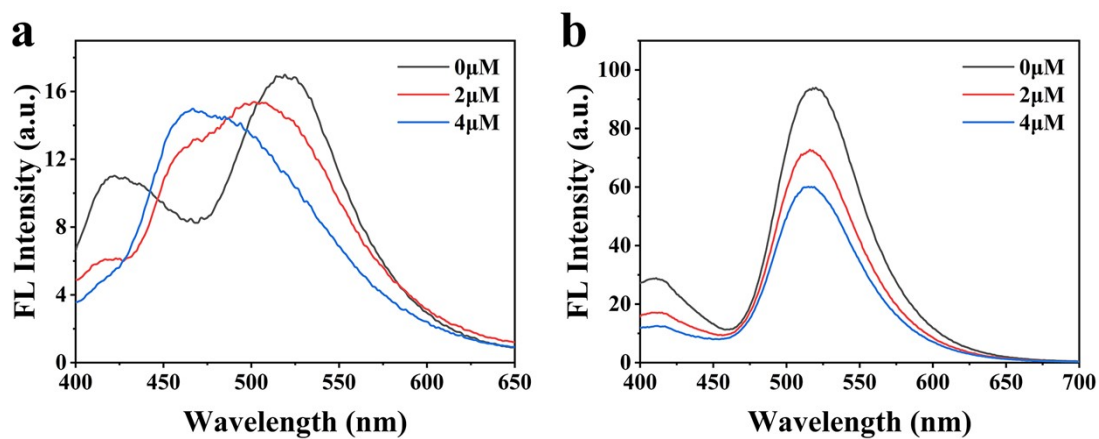


Figure S18. Fluorescence spectra of BCN (a) and 3HF (b) at low concentrations of Al³⁺

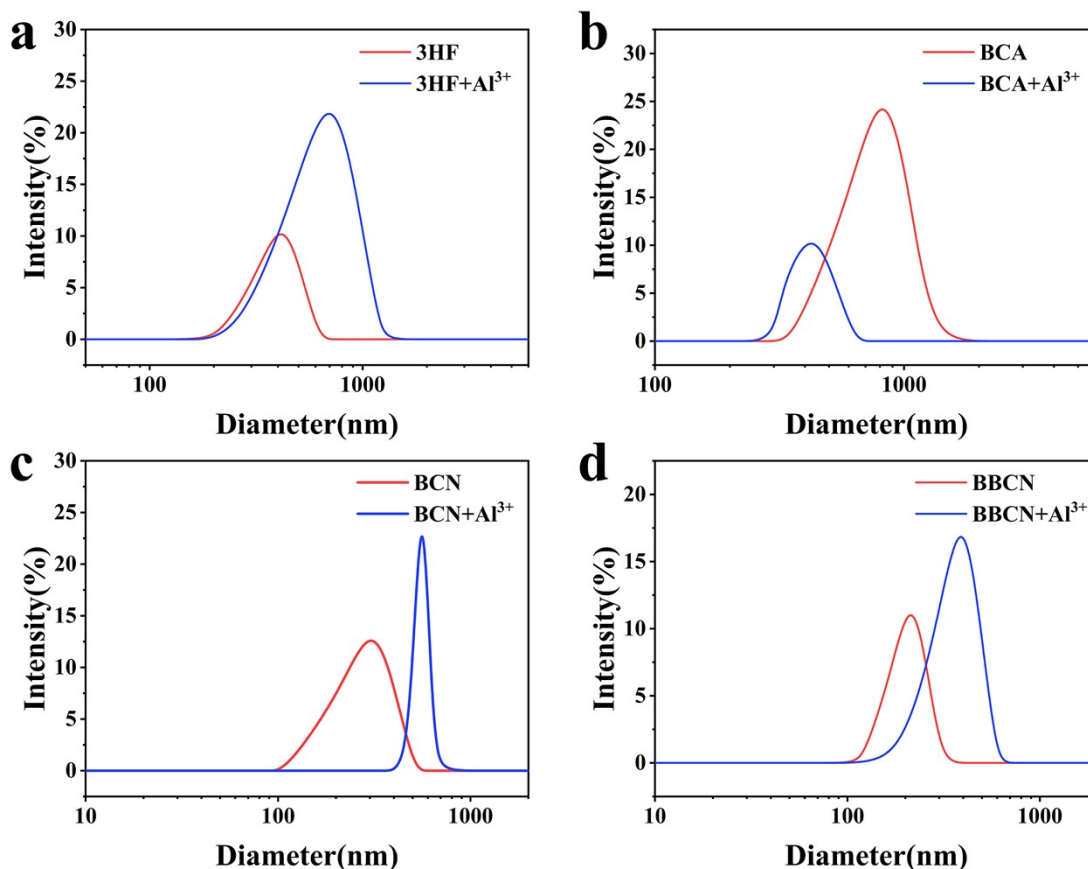


Figure S19. Size distribution(DLS) of 3HF (a), BCA (b), BCN (c), and BBCN (d) before and after adding 100 μ M of Al³⁺ in solution (H₂O:THF = 9:1).

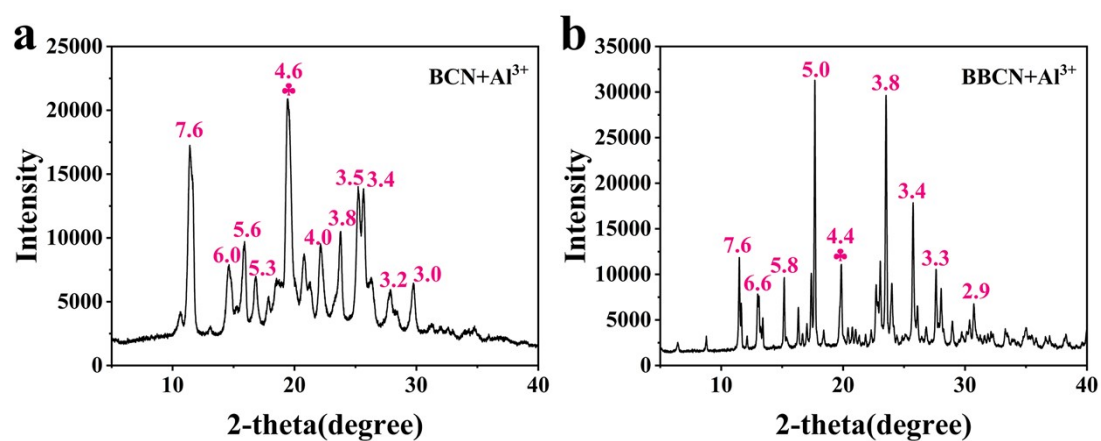


Figure S20. (a) XRD pattern of BCN-Al³⁺ and (b) XRD pattern of BBCN-Al³⁺ complexes



Figure S21. Photographs of fluorescence responses at 365 nm after adding 100 μ M different metal ions to BCN aqueous solution (H₂O:THF = 9:1).

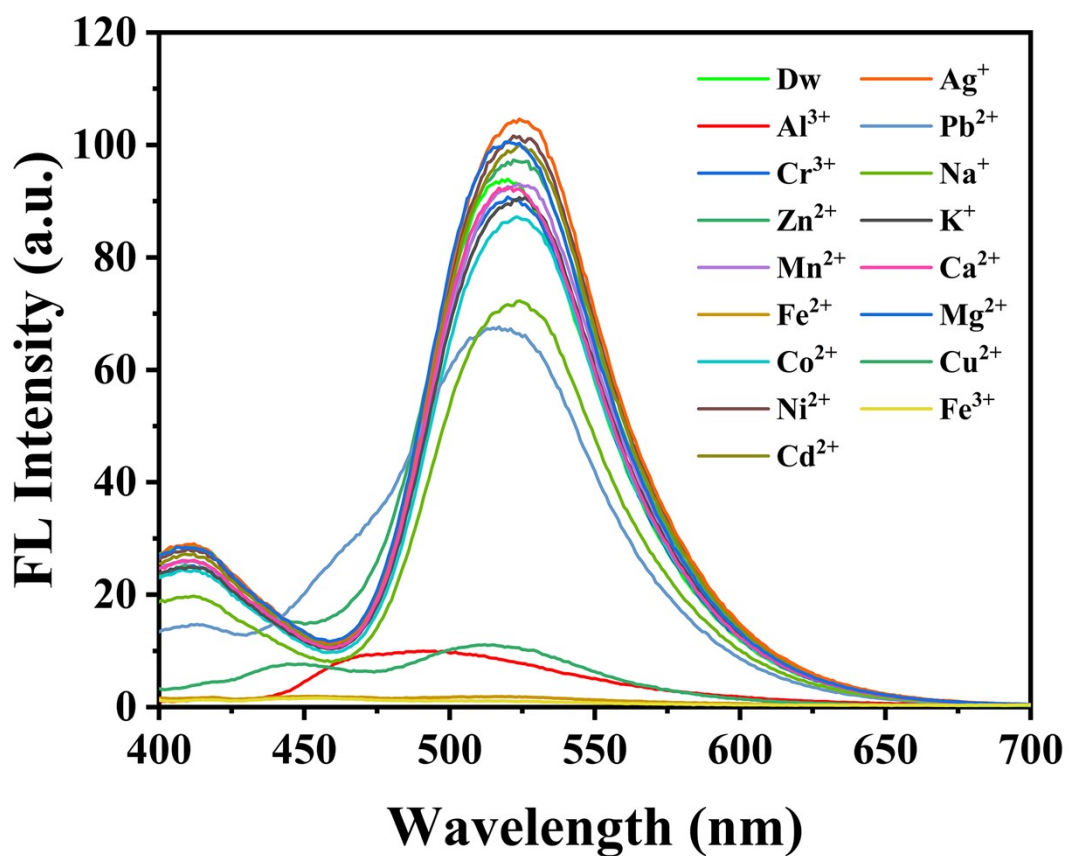


Figure S22. Fluorescence spectra of 3HF aqueous solution (H₂O:THF = 9:1) after addition of 100 μ M of various metal ions.

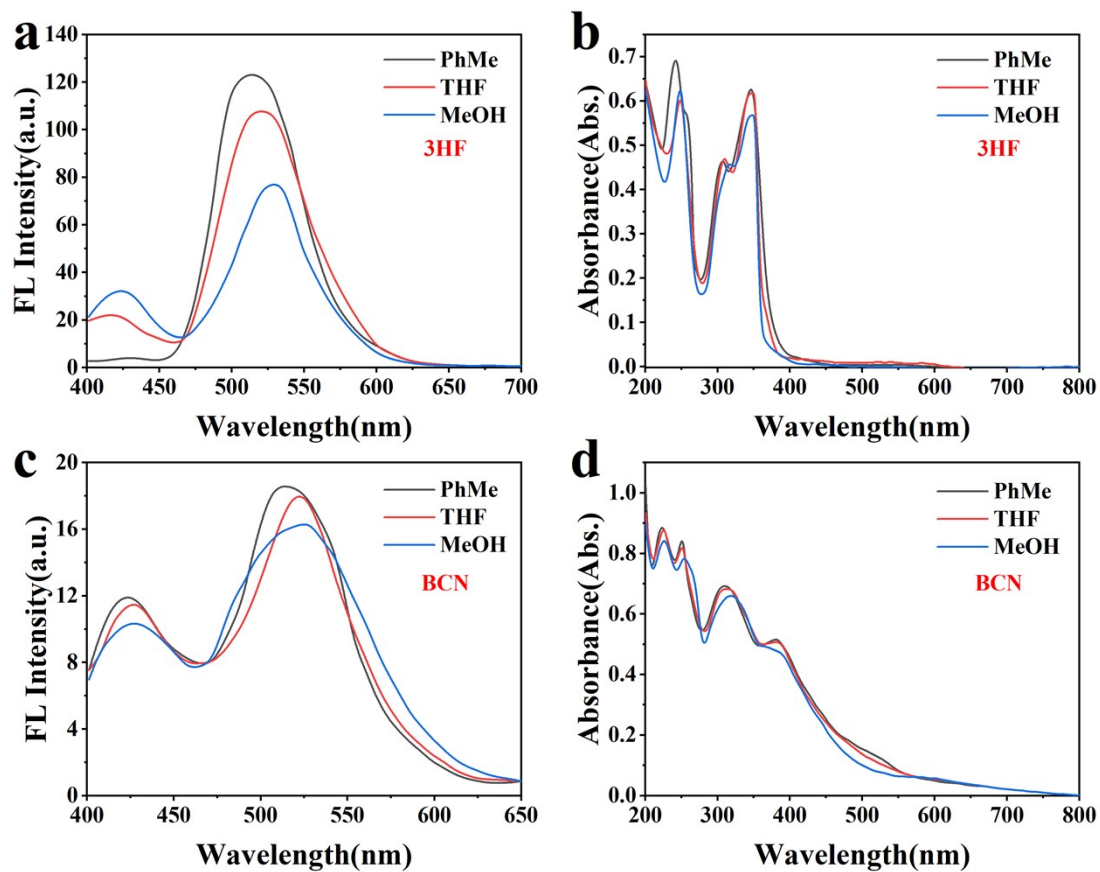


Figure S23. The photophysical behaviors of 3HF and BCN in solvents, including non-polar solvent (toluene), polar aprotic solvent (THF), and polar protic solvent (methanol).

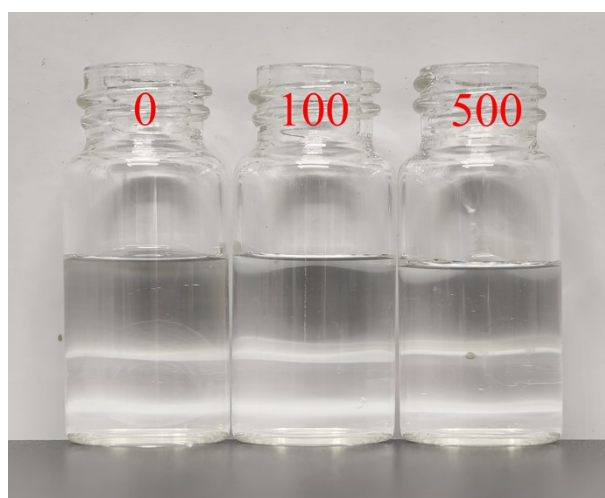


Figure S24. Color change of the system before and after adding different concentrations (0–100–500 μM) of Al^{3+} to a BCN (50 μM) aqueous solution.

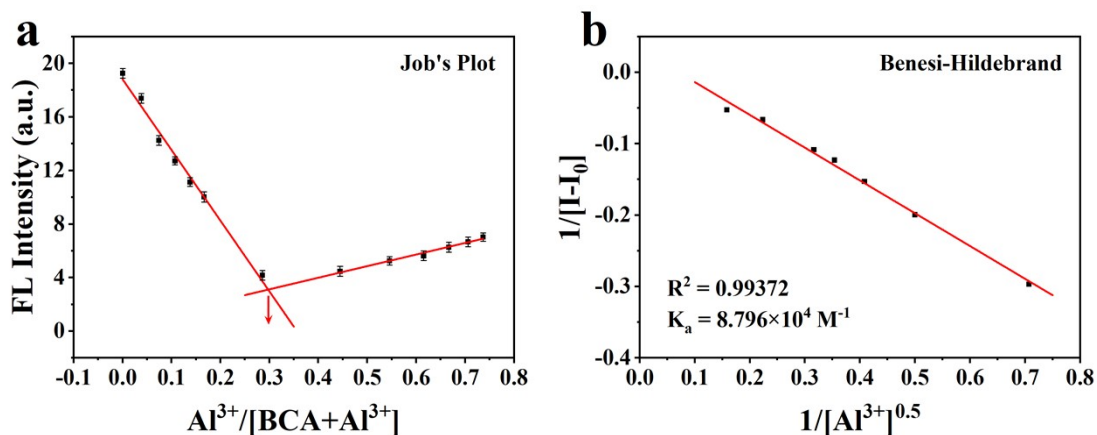


Figure S25. (a) Job curve of BCA binding to Al^{3+} in aqueous solution at a 2:1 molar ratio (all dissolution systems were $\text{H}_2\text{O}:\text{THF} = 9:1$); (b) Benesi-Hildebrand curve used to determine the binding constant.

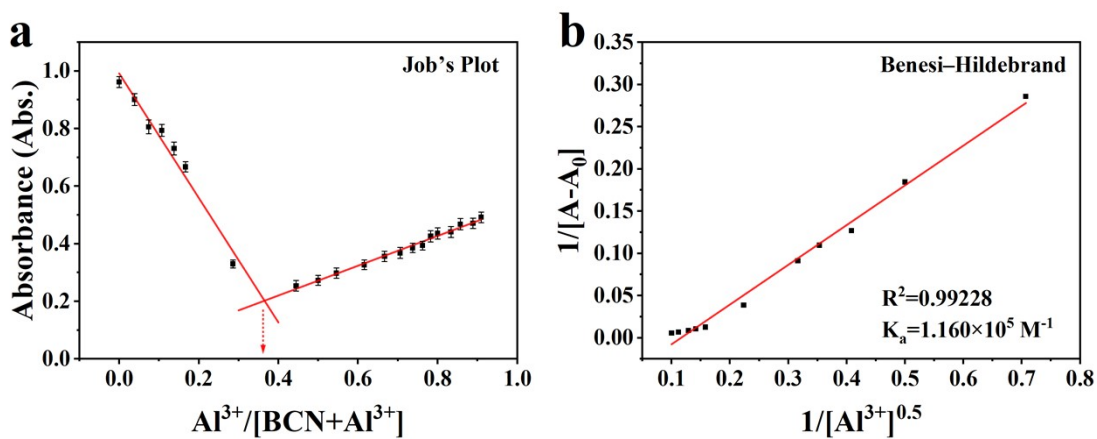


Figure S26. (a) Job curve of BCN binding to Al^{3+} in aqueous solution at a 2:1 molar ratio (all dissolution systems were $\text{H}_2\text{O}:\text{THF} = 9:1$); (b) Benesi-Hildebrand curve used to determine the binding constant.

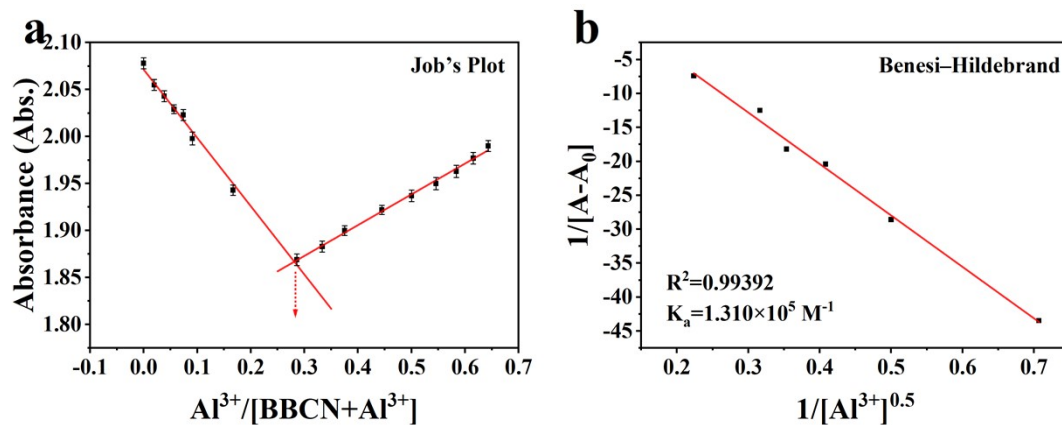


Figure S27. (a) Job curve of BBCN binding to Al^{3+} in aqueous solution at a 2:1 molar ratio (all dissolution systems were $\text{H}_2\text{O}:\text{THF} = 9:1$); (b) Benesi-Hildebrand curve used to determine the binding constant.

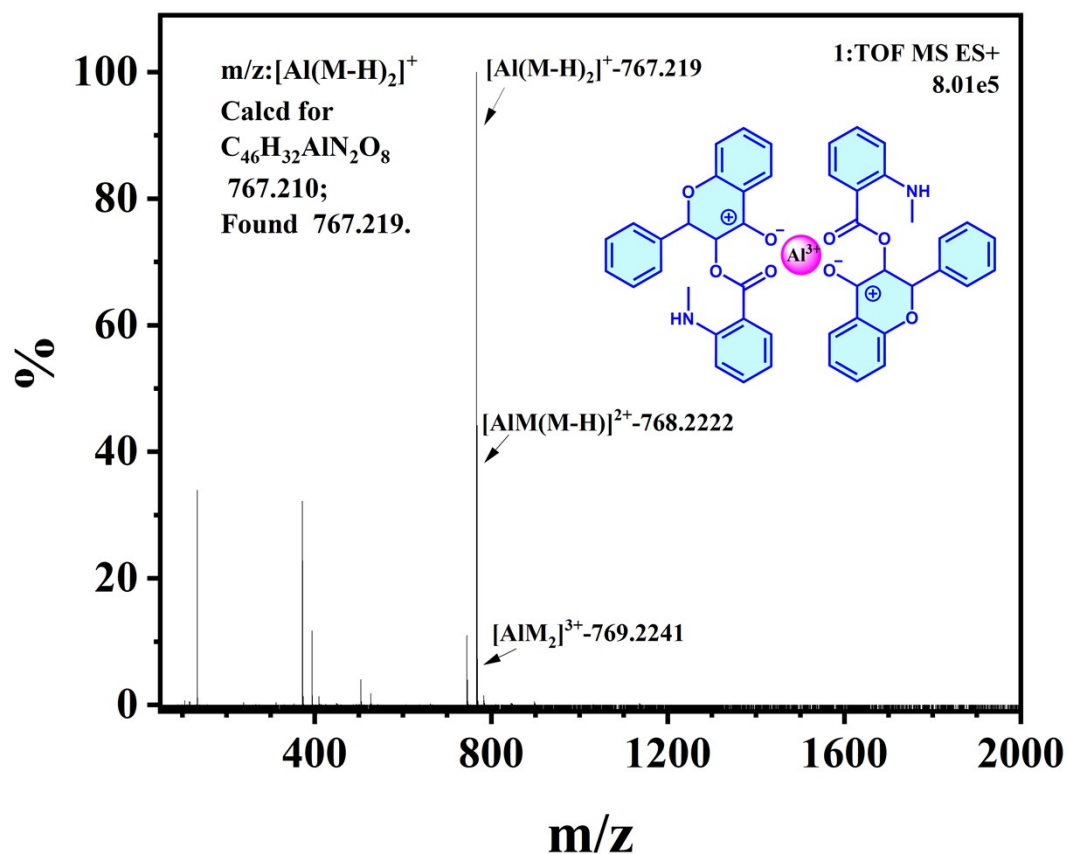


Figure S28. HRMS of $2\text{BCN}+\text{Al}^{3+}$ (ESI+).

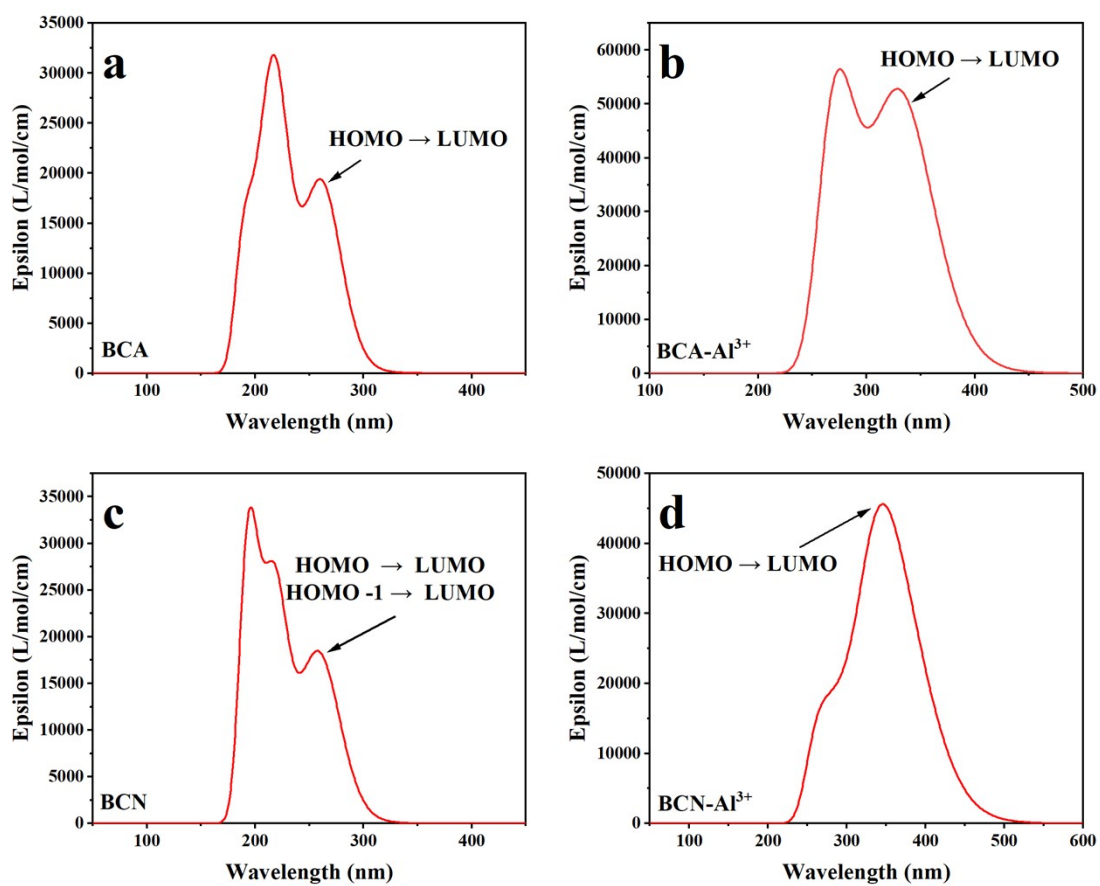


Figure S29. TD-DFT simulated absorption spectra and assignments of major electronic transitions for BCA(a), BCA-Al³⁺(b), BCN(c), and BCN-Al³⁺(d).